Intrinsic water-soluble benzoxazine-functionalized cyclodextrin and its formation of inclusion complex with polymer

Mohamed Gamal Mohamed [a], Tso Shiuan Meng [a], Shiao Wei Kuo [a,b,*]

[a] Department of Materials and Optoelectronic Science, Center of Crystal Research, National Sun Yat-Sen University, Kaohsiung, 80424, Taiwan
[b] Department of Medicinal and Applied Chemistry, Kaohsiung Medical University, Kaohsiung, 807, Taiwan

ARTICLE INFO

ABSTRACT

In this study a new water-soluble benzoxazine-functionalized cyclodextrin monomer (β-CD-BZ) was synthesized through monoazido-functionalized β-cyclodextrin (N_3-CD) with 3,4-dihydro-3-(prop-2-ynyl)-2H-benzoxazine (Ppa) by Huisgen [2 + 3] cycloadditions (click reaction) based on ^{1}H NMR and FTIR spectroscopy. Its thermal curing polymerization and thermal stability were monitored by DSC and TGA displaying the ring-opening polymerization of benzoxazine units. Incorporation of β-CD into the benzoxazine monomer could improve the thermal stability and water-solubility because of the highly hydroxyl contents of the cyclodextrin unit. Furthermore, the presence of the β-CD cavity could allow the benzoxazine monomer to form inclusion complex (IC) with poly(propylene glycol) (PPG) based on XRD, ^{1}H NMR, FTIR and TGA. From the XRD results, the PPG were confined into the β-CD-BZ channels and then form the columnar crystalline structures where the stoichiometries of repeat unit of PPG: β-CD-BZ = 2 : 1 were determined by ^{1}H NMR analysis. More importantly, the benzoxazine units in β-CD-BZ/PPG inclusion complex could further provide the thermal curing polymerization behavior to improve their thermal properties that could not be observed in typical inclusion complex system.

1. Introduction

Polybenzoxazines (PBZs) are a new class of phenolic thermosetting resins, which have garnered great interest in academic and industry fields because of their fantastic properties compared with other thermosetting resins [1–10]. It is well-known that the 1,3-benzoxazine monomers and their derivatives could be prepared through the Mannich condensation reaction of aromatic phenols, aliphatic or aromatic amines with paraformaldehyde and then thermal curing polymerization of benzoxazine monomers to afford PBZs materials, which could possess low dielectric constant; good flame retardant, adhesive strength, thermal and mechanical properties; lower surface free energy, high char yield, great flexibility of molecular design, easily thermal curing ring opening polymerization for their corresponding benzoxazine monomers without using any catalyst during polymerization, no releasing by-products and low shrinkage after polymerization [11–18]. In addition, the PBZs properties such as mechanical and thermal can be improved through addition some inorganic compounds for example, graphene, carbon nanotubes, clay and polyhedral oligomeric silsesquioxane (POSS) into PBZs matrix, or blending PBZs with polyurethane,

polyimide, and epoxy and functionalized BZ monomers with incorporation some functional groups such as nitrile, triphenyl, propargyl, allyl and phenylethynyl into BZ monomers [19–27].

Recently, PBZs have been widely used in many potential applications such as gas capture, shape-memory polymers, coating as anticorrosion materials and chelation agents for recovery of metal ions in the aqueous solution [28–33]. Recently, the new bio-based and renewable benzoxazine monomers have received particular attentions for replacing commercially inexpensive and available amine or phenols by natural products such as cardanol, eugenol, vanillin, coumaric, stearylamine and furfurylamine [7,30,34–37]. Since the intrinsic low surface free surface energy and water-repellence property because of the strong six-membered ring of OH—N intramolecular hydrogen bonding interaction of polybenzoxazine structure [38], the water-soluble benzoxazines are rarely proposed field. It is reasonable since the most researchers were mostly focused on the low water-uptake benzoxazine structure to maintain the high thermal stability and thus only a few studies can be observed in the water-soluble benzoxazine monomer. For example, Sawaryn et al. used PEO-*b*-PPO block copolymer functionalized benzoxazine monomer to tune the water solubility by changing the

---

PEO chain length [39]. Ishida et al. also used PPO-PEO-PPO triblock copolymers to synthesis water soluble main chain type of benzoxazine precursors [5]. They also proposed the chitosan-functionalized benzoxazine through the reaction of main chain type of benzoxazine with chitosan that can be soluble in acidic media [40]. Dumas et al. provided another highly hydrophilic phenol compound with an intrinsic water-affinity; arbutin is the β-D-glucoside of hydroquinone to prepare a new water soluble benzoxazine monomer with a carbohydrate moiety [34]. More interestingly, the arbutin compound also can be synthesized through glucose or through enzyme process [34,41]. In addition to arbutin compound, the well-known glucose-based molecules are the cyclodextrins (CDs), which are mainly divided into three types of compounds (called α-CD, β-CD, and γ-CD), they are cyclic oligosaccharides containing six, seven and eight glucose units connected by linked by α-1, 4 linkages and considered as receptor materials in supramolecular chemistry, respectively [42–47]. Interestingly, all CDs can form inclusion complexes with different kinds of polymers and organic compounds through their hydrophobic internal cavities by host-guest complex strategy [48–50]. In this work, the new water-soluble, highly functionalized benzoxazine with cyclodextrins, were desired to synthesize. Taking into account for the chemical structure of these three CDs, the β-CD was selected since this compound is easy to chemical modification as compared with α-CD and γ-CD as expected and widely reported [48]. The previous studies also revealed that β-CD is widely used to form inclusion complexes with other guest materials because it possesses hydrophobic cavity diameter around 0.64 nm and provide suitable hydrophobic interaction with guest molecule [48]. For example, β-CD could be formed inclusion complexes with PPG and the stoichiometries are 2:1 (two repeat units of PPG: one β-CD) based on ^{1}H NMR analysis [49,51]. The molecular model also displays that PPG chain can penetrate β-CD; however, the PPG cannot pass through the cavity of α-CD because the hindrance side chain of methyl group [51]. Therefore, a new water-soluble benzoxazine-functionalized cyclodextrin monomer (β-CD-BZ) was synthesized through monoazido-functionalized β-cyclodextrin (N₃-CD) with Ppa by click reaction as displayed in Scheme 1. Furthermore, the presence of the β-CD cavity could allow to form inclusion complex (IC) with PPG as shown in Scheme 2. More importantly, the benzoxazine units in β-CD-BZ/PPG inclusion complex could further provide the thermal curing polymerization behavior to improve their thermal properties in this study that could not be observed in typical inclusion complex.

2. Experimental section

2.1. Materials

Phenol (99.5%), propargylamine (98%), paraformaldehyde (95%),
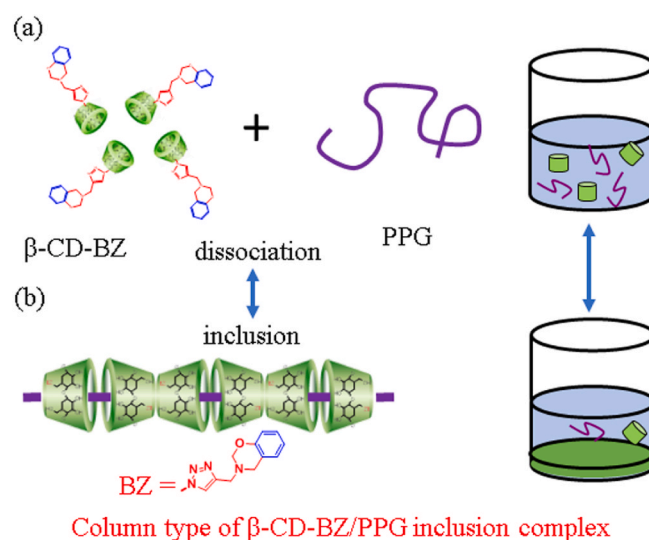
Scheme 2. Column type of β-CD-BZ/PPG inclusion complex (b) from (a) β-CD-BZ monomer with PPG homopolymer.

sodium hydroxide (NaOH, 98.5%) sodium azide (99.5%), *p*-toluenesulfonyl chloride (99.5%), poly(propylene glycol) (M_n = 1000 g/mol), copper sulfate pentahydrate (CuSO₄·5H₂O), and sodium ascorbate (NaAsc) were ordered from Sigma–Aldrich. *N,N*-dimethylformamide (DMF), diethyl ether, and acetone were purchased from Acros Organic and used without further purification. β-CD was obtained from Tokyo Kasei (Tokyo, Japan) and the preparation of mono-6-(*p*-toluenesulfonyl)-6-oxy-βCD (β-CD-Ts) was described previously [Figure S1] [50,52].

2.1.1. Preparation of mono-6-Azido-6-deoxy-βCD (β-CD-N₃) [50,52]

In two-necked round bottom flask (100 mL) under a N₂ atmosphere, β-CD-Ts (2.00 g, 1.55 mmol), NaN₃ (2.01 g, 31.10 mmol) and 50 mL of deionized H₂O and the solution mixture was heated at 90 °C for 36 h. The crude product of β-CD-N₃ was obtained through the addition of the reaction mixture to 200 mL of acetone. The obtained white solid was purified through recrystallization process by using hot water to afford β-CD-N₃ as a white solid (1.77 g, 90%). ^{1}H NMR (500 MHz, δ, ppm, DMSO-d_6): 3.47–3.15 ppm (m, 14H, –C6–H₂; overlap with HDO); 3.81–3.50 (m, 28H, C2,3,4,5–H₋), 4.63–4.37 (m, 6H, C6–OH₋), 4.94–4.76 (m, 7H, C1–H₋), 5.75 (s, 14H, C2,3–OH₋), FTIR (KBr, cm⁻¹): 3378 (O–H stretching), 2929 (C–H aliphatic stretching), 2099 (azide group, N₃), 1152 (C–O–C stretching).
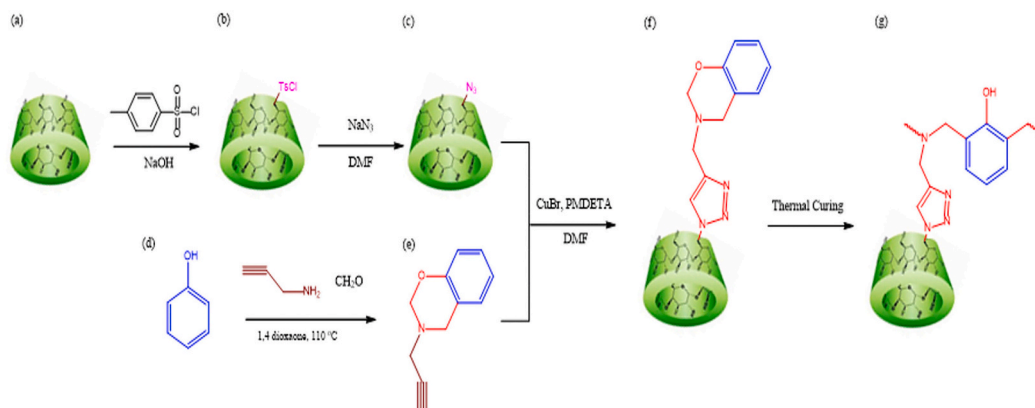
Scheme 1. Synthesis of β-CD-BZ monomer (f) by click reaction from (c) N₃-CD, prepared from (a) β-CD and (b) β-CD-Ts, with (e) Ppa, prepared from phenol (d), propargylamine and CH₂O and (g) poly(β-CD-BZ) after thermal curing polymerization of β-CD-BZ (f).

2.1.2. Synthesis of 3,4-dihydro-3-(prop-2-ynyl)-2H-benzoxazine (Ppa) [53]

In two-necked round bottom flask (100 mL) under a N_2 atmosphere, paraformaldehyde (2.18 g, 105.36 mmol), phenol (5.00 g, 52.63 mmol) and propargylamine (2.93 g, 53.13 mmol) and 50 mL of dry dioxane was stirred and refluxed at 110 °C for 24 h. The dioxane solvent was removed by rotating evaporation. Finally, the product residue was dissolved the diethyl ether and extracted three times with NaOH solution (1 N) to give Ppa as yellow viscous liquid. FTIR (KBr, cm^{-1}): 3296 (unsaturated C–H stretching), 2114 (unsaturated C–H stretching), 2925 (saturated alkyl C–H stretching), 1344 (CH_2 wagging), 1224 (C–O–C asymmetric stretching), 1110 (C–O–C symmetrical stretching), 932 (C–H out-of-plane bending). ^{1}H NMR (500 MHz, δ, ppm, DMSO-d_6): 7.33–6.75 (aromatic protons), 4.95 (O–**CH$_2$**–N), 4.23 (C–**CH$_2$**–N), 3.72 (**H$_2$C**≡CCH), 2.20 (H$_2$C≡C**CH**).

2.1.3. Preparation of benzoxazine functionalized-β-CD (β-CD-BZ) by click reaction

In two-necked round bottom flask (100 mL) under a N_2 atmosphere, β-CD-N$_3$ (3.54 g, 3.05 mmol), Ppa (0.53 g, 3.05 mmol), CuSO$_4$·5H$_2$O (0.154 g, 0.61 mmol), NaAsc (0.302 g, 1.52 mmol) was dissolved in 20 mL of dry DMF. After freeze/pump/thaw cycles for the reaction solution, the reaction mixture was heated at 50 °C for 48 h. The white solid of β-CD-BZ was precipitated using acetone (400 mL). FTIR (KBr, cm^{-1}): 3383 (O–H stretching), 1238 (C–O–C asymmetric stretching), 937(C–H out-of-plane bending). ^{1}H NMR (500 MHz, δ, ppm, DMSO-d_6): 7.94 (s, 1H, triazole ring), 7.15–6.75 (aromatic protons), 5.02 (O–**CH$_2$**–N), 4.38 (C–**CH$_2$**–N).

2.1.4. Preparation and thermal curing polymerization of β-CD-BZ/PPG inclusion complex

In a bottle (20 mL), (0.2 g, 0.190 mmol) of β-CD-BZ was dissolved in 15 mL of DI water. Then, (0.022 g, 0.380 mmol) of PPG (dissolved in 5 mL of DI H$_2$O) was added dropwise to the β-CD-BZ solution with stirring. The mixture solution was kept at 25 °C for 24 h until the white solid was formed. Finally, the white product was filtered and washed with water. 0.1 g of β-CD-BZ/PPG inclusion complex was thermally cured at 210 °C for 2 h in the oven with a heating rate 5 °C min^{-1} to afford poly(β-CD-BZ/PPG) [Scheme S1].

3. Results and discussion

3.1. Preparation of benzoxazine functionalized-β-CD (β-CD-BZ) by click reaction

In this work, the β-CD-BZ monomer was prepared through the click reaction from β-CD-N$_3$ (Scheme 1(c)) with Ppa (Scheme 1(e)) as displayed in Scheme 1. Fig. 1 displays FTIR spectra of β-CD-N$_3$, Ppa, and β-CD-BZ monomer recorded at room temperature. The azide unit of β-CD-N$_3$ was appeared at 2105 cm^{-1} and the acetylene group of Ppa was located at 3290 cm^{-1} and 2100 cm^{-1}, where were both absent in the FTIR spectrum of β-CD-BZ monomer. The remained oxazine ring of benzoxazine structure at 937 cm^{-1} and the broad absorption of the OH units of the β-CD structure at 3383 cm^{-1} also appeared in β-CD-BZ monomer, suggesting the click reaction has participated in acetylene and azido functional units.

^{1}H NMR analyses also indicate that the complete click reaction has occurred for the acetylene and azido functional units as displayed in Fig. 2. Compared with β-CD-Ts, the aromatic protons (peaks *h* and *i* in Figure S1) were disappeared in β-CD-N$_3$ and the signal of the methylene (CH$_2$) unit was shifted from 4.18 ppm (TsCl) to 3.76 ppm when connect to the N$_3$ unit of β-CD-N$_3$ (peak *g*) in Fig. 2(a). Fig. 2(c) shows ^{1}H NMR spectrum of Ppa, where the peaks at 4.92 (peak *k*) and 4.11 (peak *j*) ppm due to the CH$_2$ protons of the oxazine unit, the multiple peaks at 7.40–6.77 ppm due to the aromatic protons, and the C≡C-CH$_2$ (peak *i*) and C≡CH$_2$ (peak *h*) and were located at 3.60 and 2.30 ppm. Compared
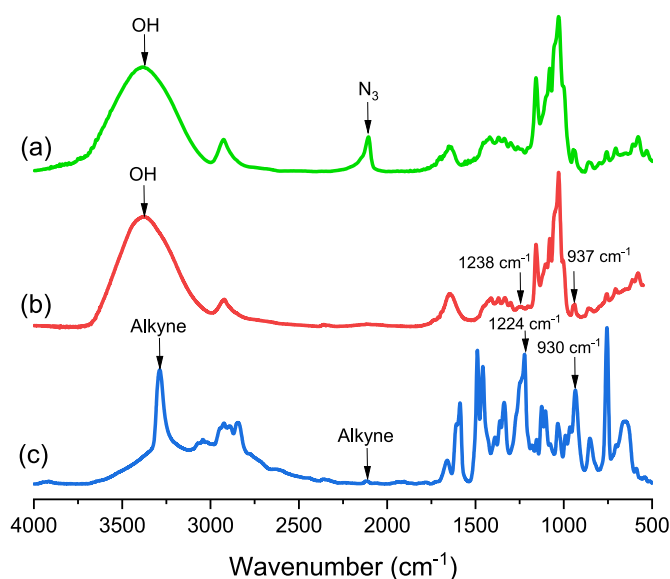
Fig. 1. FTIR spectra of (a) N$_3$-CD, (b) β-CD-BZ and (c) Ppa recorded at room temperature.

with β-CD-N$_3$ and Ppa, we clearly observed that the CH$_2$ unit at 3.76 ppm was downfield to 3.93 ppm (peak *g*) and the new signal at 7.95 ppm (peak *h*) for β-CD-BZ monomer in Fig. 2(b), which was corresponding to the triazole structure after the click reaction and the peaks at 5.02 and 4.27 ppm were shifted from the methylene bridge (4.92 and 4.11 ppm) of the oxazine ring. More importantly, the peak intensity ratio of peaks *k* and *j* was 1:1 and also consistent with the aromatic protons ratio, which were remained at 7.40–6.77 ppm in Fig. 2(b). Taken the FTIR and NMR result together, it was confirmed the successful synthesis of β-CD-BZ monomer under the click reaction.

3.2. Thermal curing polymerization of β-CD-BZ monomer

We investigated the thermal curing polymerization behavior of Ppa and β-CD-BZ monomer by DSC analyses. Fig. 3(a) shows the DSC profile of pure Ppa benzoxazine, which possesses a maximum exotherm at 212 °C with the exotherm reaction heat of 1087 J/g. The DSC thermogram of β-CD-BZ displays an exotherm peak at 229 °C and the corresponding exotherm reaction heat was 44.3 J/g. Clearly, the reaction heat was significantly decreased after the incorporation of β-CD unit, which strongly affect the thermal curing behavior of the benzoxazine monomer because of the dilution effect and the loss of propargyl unit from the Ppa monomer [53–55]. In general, DSC analyses and FTIR spectra could be used to understand the thermal curing polymerization of the β-CD-BZ monomer.

As shown in Fig. 4(A) about DSC analyses, the uncured β-CD-BZ monomer exhibits the maximum exotherm at 229 °C with the reaction heat of 44.3 J/g as mentioned in Fig. 3(a). The bulk CD unit is difficult to ring-opening of the oxazine ring (T_p = 229 °C) as compared with Ppa benzoxazine (T_p = 212 °C) as expected. After thermal curing at different temperatures from 110 to 210 °C, the curing exothermic peak of β-CD-BZ monomer was gradually shifted to higher temperature and the reaction heat was also gradually decreased with the increase of curing temperature. In addition, the curing peak was completely disappeared after thermal curing temperature at 210 °C, implying the thermal curing polymerization of β-CD-BZ completed at 210 °C. The corresponding FTIR spectra of β-CD-BZ after each curing stage was summarized in Fig. 4(B) to understand its ring-opening polymerization behavior from 25 to 210 °C. Clearly, the oxazine ring of benzoxazine structure at 937 cm^{-1} and 1157 cm^{-1} were progressively consumed with the increase of curing temperature and then totally disappeared at 210 °C, which is
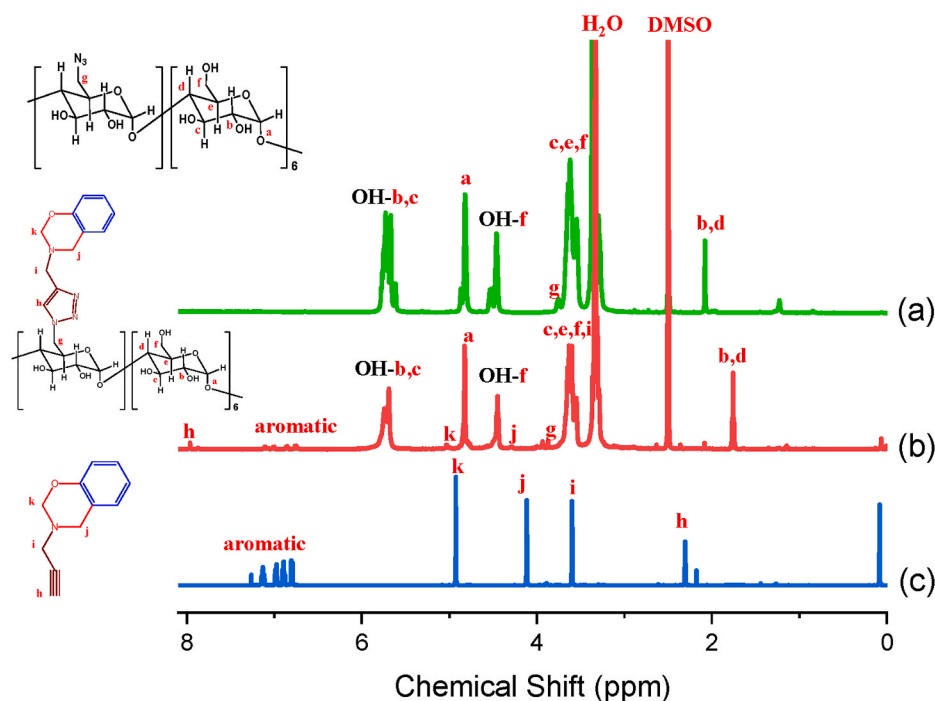
Fig. 2. ^{1}H NMR spectra of (a) N$_3$-CD, (b) β-CD-BZ and (c) Ppa.
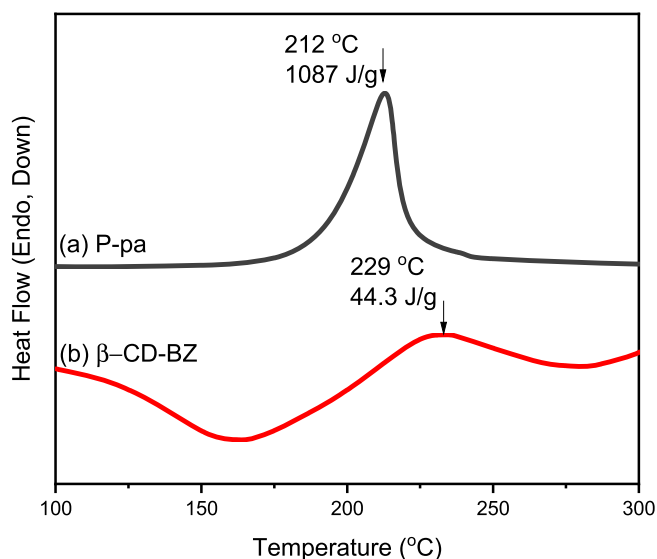
Fig. 3. First heating scan of (a) Ppa and (b) β-CD-BZ monomers.

consistent with DSC analyses.

The ring-opening polymerization of β-CD-BZ also could monitor by ^{1}H NMR spectra as shown in Fig. 5 since CD unit could provide better solubility in water or organic solvent. After thermal curing at 180 °C, the NMR spectra exhibit the appearance of three new signals at 5.30, 4.11, and 3.16 ppm, which are corresponding to the phenolic OH group, Mannich bridge of ring-opened BZ structure (peaks l and m), respectively [34]. This result could be demonstrated the ring-opening polymerization of β-CD-BZ and the FITR spectra (Fig. 4(B)) provide the good accordance with this observation, the increase of band absorption at 1730 cm^{-1} is due to the intermolecular hydrogen bonding interaction of polybenzoxazine structure[34] and the final possible ring opening structure was shown in Scheme 1(g).

The thermal decomposition temperature at 10 wt% loss (T_{d10}) and char yield at 700 °C (weight residue) of β-CD-BZ based on TGA analyses as displayed in Fig. 6(a). Because the thermal curing polymerization was occurred of the β-CD-BZ, the T_{d10} and char yield were increased upon increasing the thermal curing temperature by the increase of cross-linking density as summarized in Fig. 6(b). Furthermore, the T_{d10} and char yield were significantly increased from 236 °C to 12.4 wt% of un-cured sample to 372 °C and 54.9 wt% after thermal treatment at 300 °C. As compared with the thermal properties of typical Pa type of benzox-azine, the T_{d10} and char yield are 264 °C and 43.2 wt% at 700 °C [56], and thus the better thermal stability was observed of our new β-CD-BZ after thermal curing polymerization process.

3.3. Preparation and thermal curing polymerization of β-CD-BZ/PPG inclusion complex

The cross-section area or side chain units of polymer is well-known closed to the cavity size the cyclodextrins to form the inclusion com-plex. The β-CD inclusion complexes with linear PPG could be formed in reasonable yield, but PPG could not form inclusion complex with α-CD and γ-CD has been widely investigated [51,57]. We used β-CD or β-CD-BZ aqueous solution with the PPG aqueous solution as shown in Scheme 2.

The crystalline inclusion complexes have been observed since the solution progressively becomes turbid, suggesting the formation of ICs between the PPG and β-CD or β-CD-BZ. We then used the water to remove the uncomplexed PPG and β-CD or β-CD-BZ of ICs. In general, the crystalline inclusion complex structure could be determined by wide-angle X-ray diffraction (WAXD) as shown in Fig. 7. Firstly, there are many peaks for pure β-CD with rather distinct and sharp and then the first, second and third strongest peaks of pure β-CD were observed at 12.4, 18.6, and 10.5°, implying that the β-CD possesses the typical cage type crystalline structure (Scheme 2(a)). Different from with pure β-CD, the β-CD/PPG inclusion complex provides the first, second and third strongest peaks at 17.5, 11.4, and 6.5°. The d-spacing was calculated based on the peak ratios of these peaks are $1:\sqrt{3}:\sqrt{7}$, indicating that hexagonal lateral packing of molecular columns, which is completely different with the cage-type structure of pure β-CD [58–60]. Similar pattern was observed for the β-CD-BZ/PPG inclusion complex where the
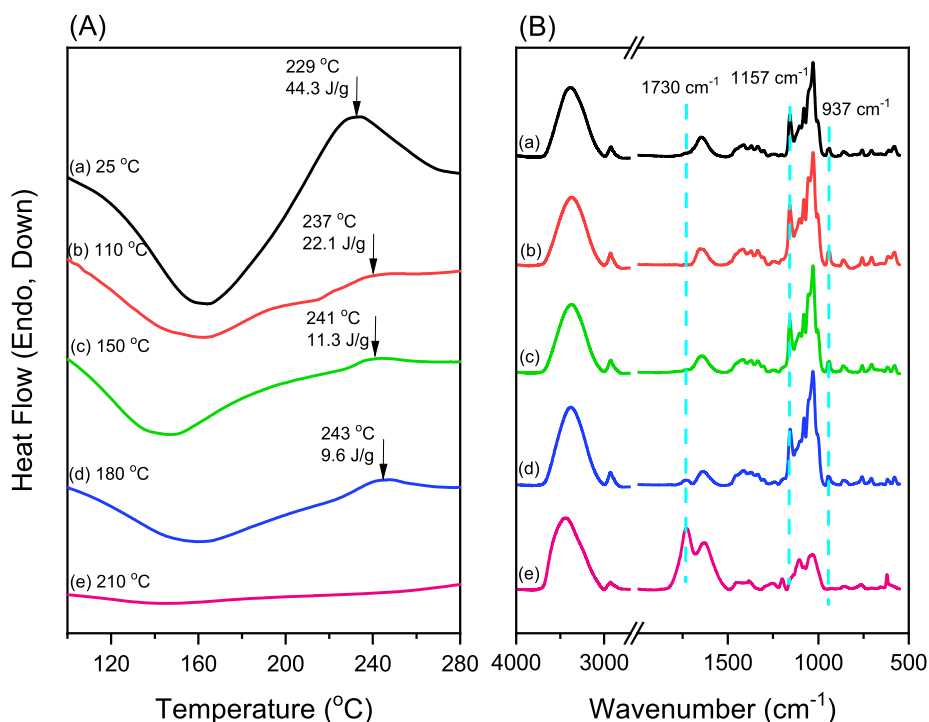
Fig. 4. (A) DSC and (B) FTIR analyses of β-CD-BZ after thermal curing at each temperature.
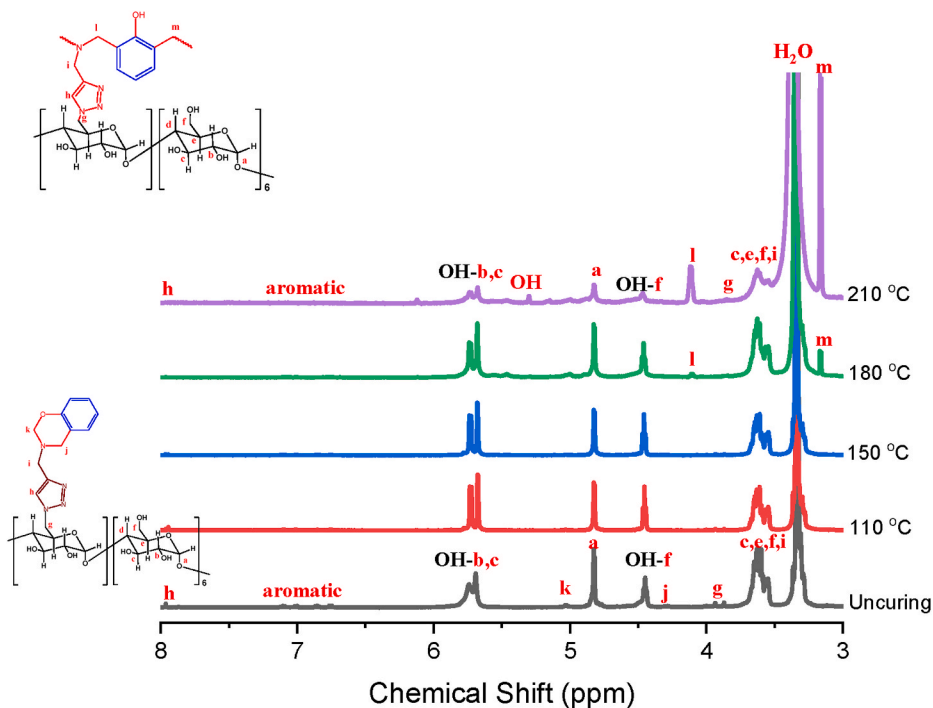
Fig. 5. ^{1}H NMR spectra of β-CD-BZ after thermal curing at each temperature.

three strongest peaks are also observed at 17.5, 11.4, and 6.5°, which is similar with β-CD/PPG inclusion complex. The broader peaks were observed in β-CD-BZ/PPG inclusion complex, implying that the crystalline structure was slightly destroyed since the one of hydroxyl units was modified to benzoxazine ring and it will affect the of hydroxyl-hydroxyl units between primary-primary (head-to-head) and secondary-secondary (tail to tail) intermolecular hydrogen bonding interactions [51]. As a result, it could be proposed that the β-CD or

β-CD-BZ units are vertically stacked with the PPG polymers in the channel-type structure (Scheme 2(b)).

The composition of the β-CD-BZ/PPG inclusion complex could be determined by ^{1}H NMR spectroscopy a shown in Fig. 8. ^{1}H NMR spectrum of pure β-CD-BZ (Fig. 8(a)) has been discussed in Fig. 2(b). Fig. 8(b) shows ^{1}H NMR spectrum of the β-CD-BZ/PPG inclusion complex, which is corresponding to both pure β-CD-BZ and PPG homopolymer. Pure PPG shows the side chain methyl (CH$_3$) units at 1.030 ppm which has been
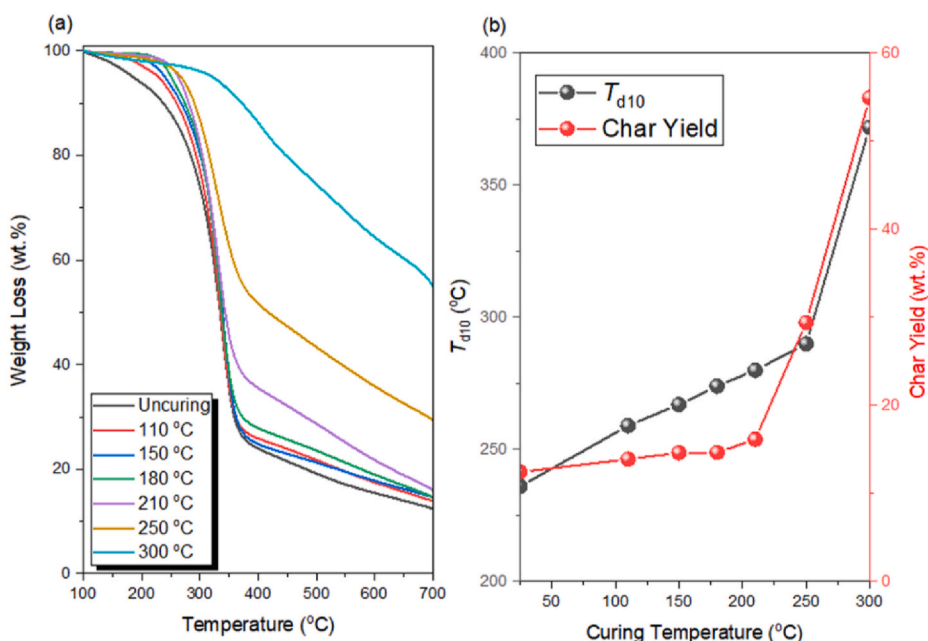
Fig. 6. (A) TGA analyses and (B) thermal stability of β-CD-BZ monomer determined after each curing temperature.
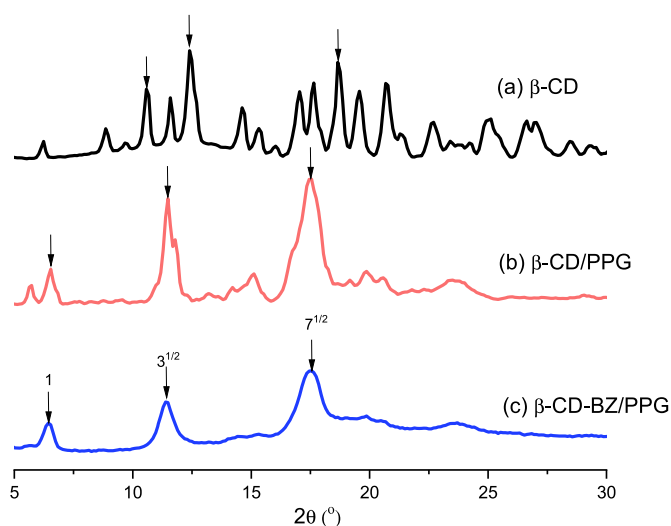
Fig. 7. XRD analyses of (a) β-CD, (b) β-CD/PPG IC, and (c) β-CD-BZ/PPG IC.

proposed and pure β-CD-BZ displays the protons (peaks **b** and **d**) at 1.756 ppm as mentioned in Fig. 2(b). Clearly, the methyl group of PPG was become broader at 1.030 ppm and the peaks **b** and **d** was significantly shifted downfield to 2.082 ppm, but the other protons of β-CD-BZ did not change, showing a possible complexation interaction in cavity of β-CD-BZ with PPG homopolymer [43,59,60]. As compared with the integral area ratio of the PPG methyl units and the peak **a** proton of β-CD-BZ, we could calculate the average of ca. 2 propylene oxide repeat units of PPG to one β-CD-BZ, which is similar with the β-CD/PPG inclusion complexes [51]. More importantly, the peaks at 5.02 and 4.27 ppm from the methylene bridge of the oxazine ring and the triazole proton (7.95 ppm) and aromatic protons (7.40–6.77 ppm) were maintained, indicating that β-CD-BZ/PPG inclusion complex could further provide the thermal curing polymerization behavior to improve their thermal properties.

Fig. 9 shows FTIR and TGA analyses to further strong evidence of the β-CD-BZ/PPG inclusion complex. Clearly, the FTIR spectrum of the β-CD-BZ/PPG inclusion complex (Fig. 9(A)) exhibits both β-CD-BZ and

PPG absorptions, implying that both components are present in the inclusion complex. The broad OH absorption of β-CD-BZ at ca. 3383 cm^{-1} was shifted to 3354 cm^{-1} in the β-CD-BZ/PPG inclusion complex due to the non-covalent interaction between β-CD-BZ and PPG main chain, which is consistent with ^{1}H NMR analysis. The inclusion complex is also thermal stable, which is supported by TGA analyses as shown in Fig. 9 (B). Clearly, the β-CD-BZ/PPG inclusion complex shows the thermal decomposition temperature at 10 wt% loss (T_{d10} = 289 °C) and char yield at 700 °C (7.3 wt%) between pure β-CD-BZ (T_{d10} = 236 °C and char yield = 12.4 wt%) and pure PPG (T_{d10} = 318 °C and char yield = 0.1 wt %) as expected. In addition, β-CD-BZ/PPG inclusion complex undergoes three-step thermal degradation. The first mass loss about 3.0 wt% in the 100–200 °C is corresponding to the water absorption [60], the second step in the 200–400 °C is assigned to the mainly decomposition of PPG segment and the final step (>400 °C) is mainly that of β-CD-BZ. The thermal stability of β-CD-BZ/PPG inclusion complex is higher than pure β-CD-BZ, implying that the addition of PPG polymer into the β-CD-BZ channels could improve the thermal stability of original β-CD-BZ [59, 60].

Furthermore, since the β-CD-BZ/PPG inclusion complex with benzoxazine units could further provide the thermal curing polymerization behavior to improve their thermal properties, we also used TGA analyses to investigate the thermal stability of β-CD-BZ/PPG inclusion complex before and after thermal curing behavior as displayed in Fig. 10. Compared with β-CD/PPG inclusion complex (T_{d10} = 335 °C and char yield = 1.6 wt% at 700 °C) as shown in Fig. 10(a), the β-CD-BZ/PPG inclusion complex shows the T_{d10} = 289 °C and char yield at 700 °C (7.3 wt%) in Fig. 10(b). The attached alkyl methylene, triazole and benzoxazine units of β-CD-BZ may possess the lower thermal decomposition temperature compared with pure β-CD; however, the thermal curing of β-CD-BZ/PPG inclusion complex could enhance the thermal stability to T_{d10} = 296 °C and char yield at 700 °C (13.8 wt%). As a result, the benzoxazine unit into the β-CD could enhance the thermal stability, especially in char yield because of thermal curing polymerization behavior of benzoxazine unit and this study provides another approach about the CD inclusion complex with high thermal stability.

4. Conclusions

A new water-soluble benzoxazine-functionalized cyclodextrin
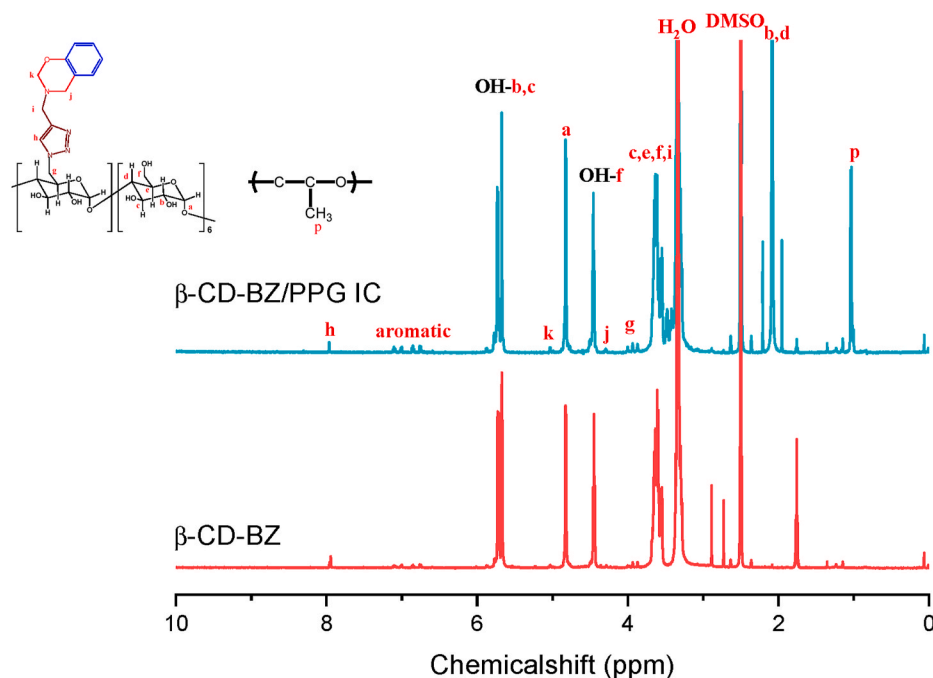
Fig. 8. ¹H NMR spectra of β-CD-BZ and β-CD-BZ/PPG IC dissolved in DMSO-d_6.
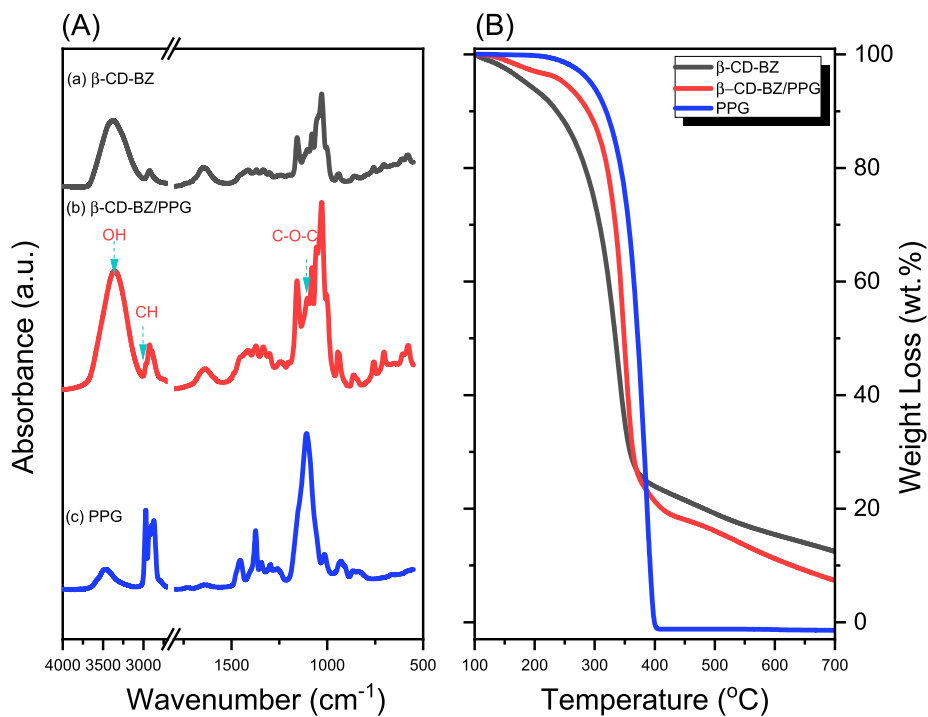
Fig. 9. (A) FTIR and (B) TGA analyses of β-CD-BZ, PPG and β-CD-BZ/PPG IC.

monomer was successfully prepared starting from the novel monoazido-functionalized β-cyclodextrin with Ppa through a click reaction. The good water solubility is due to the high concentration of hydroxyl content of cyclodextrin unit and the TGA analyses revealed that the decomposition temperatures of β-CD-BZ improved by incorporating β-CD. More importantly, the presence of the β-CD cavity could allow forming inclusion complex with PPG into the columnar crystalline structures and then the benzoxazine units in β-CD-BZ/PPG inclusion complex could further provide the thermal curing polymerization behavior to improve their thermal properties again.

CRediT authorship contribution statement

Mohamed Gamal Mohamed: Methodology, Conceptualization, Data curation, Investigation, Writing – original draft. **Tso Shiuan Meng:** Methodology, Conceptualization, Data curation, Investigation. **Shiao Wei Kuo:** Conceptualization, Methodology, Data curation, Writing – review & editing.
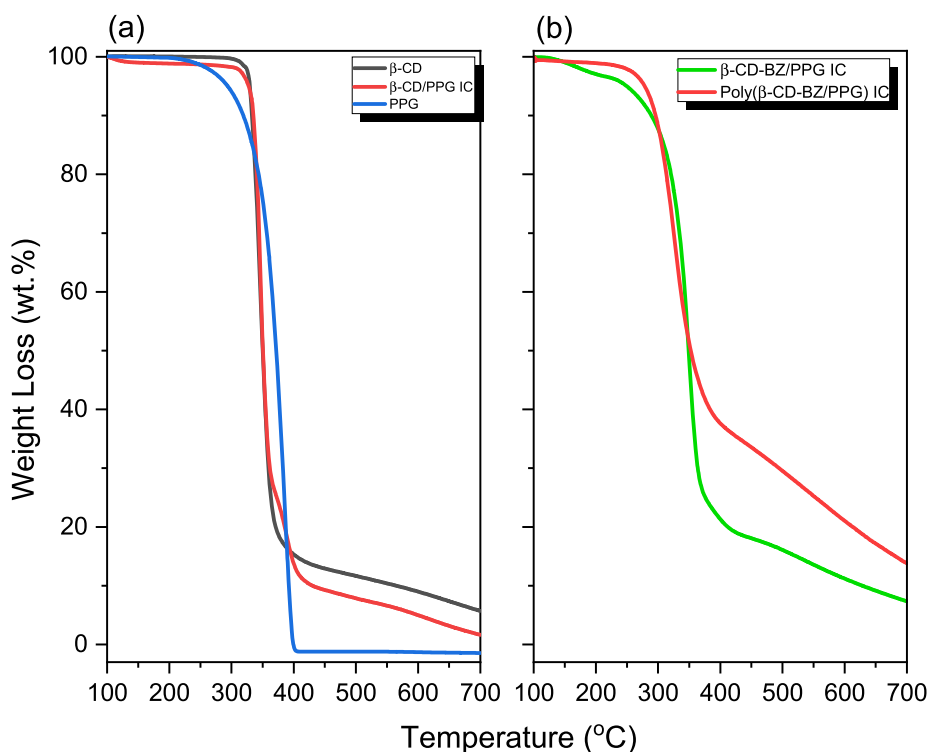
Fig. 10. TGA analyses of (a) β-CD, PPG, and β-CD/PPG IC and (b) β-CD-BZ/PPG and poly(β-CD-BZ/PPG) ICs.

Declaration of competing interest

The authors declare the following financial interests/personal relationships which may be considered as potential competing interests:

Acknowledgments

Appendix A. Supplementary data

Supplementary data to this article can be found online at https://doi.org/10.1016/j.polymer.2021.123827.

References

[1] N. Yadav, M. Monisha, R. Niranjan, A. Dubey, S. Patil, R. Priyadarshini, B. Lochab, Antibacterial performance of fully biobased chitosan-grafted-polybenzoxazine films: elaboration and properties of released material, Carbohydr. Polym. 254 (2021) 117296.

[2] Y. Lyu, E. Rachita, N. Pogharian, P. Froimowicz, H. Ishida, Electronic effects of asymmetric and meta-alkoxy substituents on the polymerization behavior of bis-benzoxazines, Polym. Chem. 11 (2020) 800–809.

[3] X. Zhang, M.G. Mohamed, Z. Xin, S.W. Kuo, A tetraphenylethylene-functionalized benzoxazine and copper(II) acetylacetonate form a high-performance polybenzoxazine, *Polymer* 201 (2020) 122552.

[4] A.A. Alhwaige, H. Ishida, S. Qutubuddin, Poly(benzoxazine-f-chitosan) films: the role of aldehyde neighboring groups on chemical interaction of benzoxazine precursors with chitosan, Carbohydr. Polym. 209 (2019) 122–129.

[5] T. Agag, S. Geiger, S.M. Alhassan, S. Qutubuddin, H. Ishida, Low-viscosity polyether based main-chain benzoxazine polymers: precursors for flexible thermosetting polymers, Macromolecules 43 (2010) 7122–7127.

[6] M.G. Mohamed, S.W. Kuo, Crown ether-functionalized polybenzoxazine for metal ion adsorption, Macromolecules 53 (2020) 2420–2429.

[7] M.M. Samy, M.G. Mohamed, S.W. Kuo, Directly synthesized nitrogen-and-oxygen–doped microporous carbons derived from a bio-derived polybenzoxazine exhibiting high-performance supercapacitance and CO₂ uptake, Eur. Polym. J. 138 (2020) 109954.

[8] M.G. Mohamed, M.Y. Tsai, W.C. Su, A.F.M. EL-Mahdy, C.F. Wang, C.F. Huang, L. Dai, T. Chen, S.W. Kuo, Nitrogen-Doped microporous carbons derived from

[9] K.I. Aly, M.G. Mohamed, O. Younis, M.H. Mahross, M.A. Hakim, M.M. Sayed, Salicylaldehyde azine-functionalized polybenzoxazine: synthesis, characterization, and its nanocomposites as coatings for inhibiting the mild steel corrosion, Prog. Org. Coating 138 (2020) 105385.

[10] S. Ohashi, E. Rachita, S. Baxley, J. Zhou, A. Erlichman, H. Ishida, The first observation on polymerization of 1,3-benzothiazines: synthesis of mono- and bis-thiazine monomers and thermal properties of their polymers, Polym. Chem. 12 (2021) 379–388.

[11] M.G. Mohamed, C.H. Hsiao, K.C. Hsu, F.H. Lu, H.K. Shih, S.W. Kuo, Supramolecular functionalized polybenzoxazines from azobenzene carboxylic acid/azobenzene pyridine complexes: synthesis, surface properties, and specific interactions, RSC Adv. 5 (2015) 12763–12772.

[12] M.M. Samy, M.G. Mohamed, S.W. Kuo, Pyrene-functionalized tetraphenylethylene polybenzoxazine for dispersing single-walled carbon nanotubes and energy storage, Compos. Sci. Technol. 199 (2020) 108360.

[13] H.R. Abuzeid, A.F.M. EL-Mahdy, M.M.M. Ahmed, S.W. Kuo, Triazine-functionalized covalent benzoxazine framework for direct synthesis of N-doped microporous carbon, Polym. Chem. 10 (2019) 6010–6020.

[14] K. Zhang, X. Yu, S.W. Kuo, Outstanding dielectric and thermal properties of main chain-type poly(benzoxazine-co-imide-co-siloxane)-based cross-linked networks, Polym. Chem. 10 (2019) 2387–2396.

[15] B. Hao, L. Han, Y. Liu, K. Zhang, An apigenin-based bio-benzoxazine with three polymerizable functionalities: sustainable synthesis, thermal latent polymerization, and excellent thermal properties of its thermosets, Polym. Chem. 11 (2020) 5800–5809.

[16] S.N. Kolanadiyil, M. Minami, T. Endo, Implementation of meta-positioning in tetrafunctional benzoxazines: synthesis, properties, and differences in the polymerized structure, Macromolecules 53 (2020) 6866–6886.

[17] Z. Deliballi, B. Kiskan, Y. Yagci, Advanced polymers from simple benzoxazines and phenols by ring-opening addition reactions, Macromolecules 53 (2020) 2354–2361.

[18] A.F.M. EL-Mahdy, F.W. Lin, W.H. Su, T. Chen, S.W. Kuo, Photoresponsive azobenzene materials based on pyridine-functionalized benzoxazines as surface relief gratings, ACS Appl. Polym. Mater. 2 (2020) 791–804.

[19] R. Tavernier, L. Granado, G. Foyer, G. David, S. Caillol, Formaldehyde-free polybenzoxazines for high performance thermosets, Macromolecules 53 (2020) 2557–2567.

[20] M.G. Mohamed, S.W. Kuo, Functional silica and carbon nanocomposites based on polybenzoxazines, Macromol. Chem. Phys. 220 (2019) 1800306.

[21] M.G. Mohamed, S.W. Kuo, A. Mahdy, I.M. Ghayd, K.I. Aly, Bisbenzylidene cyclopentanone and cyclohexanone-functionalized polybenzoxazine nanocomposites: synthesis, characterization, and use for corrosion protection on mild steel, Mater. Today Commun. 25 (2020) 101418.

azobenzene and nitrile-functionalized polybenzoxazines for CO2 uptake, Mater. Today Commun. 24 (2020) 101111.

[22] K.I. Aly, A. Mahdy, M.A. Hegazy, N.S. Al-Muaikel, S.W. Kuo, M.G. Mohamed, Corrosion resistance of mild steel coated with phthalimide-functionalized polybenzoxazines, Coatings 10 (2020) 1114.

[23] M.G. Mohamed, S.M. Ebrahium, A.S. Hammam, S.W. Kuo, K.I. Aly, Enhanced CO_2 capture in nitrogen-enriched microporous carbons derived from Polybenzoxazines containing azobenzene and carboxylic acid units, J. Polym. Res. 27 (2020) 197.

[24] W.C. Chen, S.W. Kuo, Ortho-Imide and allyl groups effect on highly thermally stable polybenzoxazine/double-decker-shaped polyhedral silsesquioxane hybrids, Macromolecules 51 (2018) 9602–9612.

[25] M.G. Mohamed, C.H. Hsiao, F. Luo, L. Dai, S.W. Kuo, Multifunctional polybenzoxazine nanocomposites containing photoresponsive azobenzene units, catalytic carboxylic acid groups, and pyrene units capable of dispersing carbon nanotubes, RSC Adv. 5 (2015) 45201–45212.

[26] Y.T. Liao, Y.C. Lin, S.W. Kuo, Highly thermally stable, transparent, and flexible polybenzoxazine nanocomposites by combination of double-decker-shaped polyhedral silsesquioxanes and polydimethylsiloxane, Macromolecules 50 (2017) 5739–5747.

[27] R.C. Lin, M.G. Mohamed, S.W. Kuo, Benzoxazine/triphenylamine-based dendrimers prepared through facile one-pot Mannich condensations, Macromol. Rapid Commun. 38 (2017) 1700251.

[28] R. Tavernier, L. Granado, G. Foyer, G. David, S. Caillol, Aromatic dialdehyde-based bisbenzoxazines: the influence of relative position of oxazine rings, Polymer 216 (2021) 123270.

[29] M. Ohara, K. Yoshimoto, T. Kawauchi, T. Takeichi, Synthesis of high-molecular-weight benzoxazines having azomethine linkages in the main-chain and the properties of their thermosetting resins, Polymer 202 (2020) 122668.

[30] M.G. Mohamed, K.C. Hsu, S.W. Kuo, Bifunctional polybenzoxazine nanocomposites containing photo-crosslinkable coumarin units and pyrene units capable of dispersing single-walled carbon nanotubes, Polym. Chem. 6 (2015) 2423–2433.

[31] X. Li, Y. Liu, H. Chen, H. Li, Benzoxazine monomers containing triphenylimidazole: polymerization of monomers and properties of polybenzoxazines, Eur. Polym. J. 121 (2019) 109347.

[32] M.G. Mohamed, S.W. Kuo, Polybenzoxazine/polyhedral oligomeric silsesquioxane (POSS) nanocomposites, Polymers 8 (2016) 225.

[33] J.Y. Wu, M.G. Mohamed, S.W. Kuo, Directly synthesized nitrogen-doped microporous carbons from polybenzoxazine resins for carbon dioxide capture, Polym. Chem. 8 (2017) 5481–5489.

[34] L. Dumas, L. Bonnaud, M. Olivier, M. Poorteman, P. Dubois, Arbutin-based benzoxazine: en route to an intrinsic water-soluble biobased resin, Green Chem. 18 (2016) 4954–4960.

[35] C.F. Wang, J.Q. Sun, X.D. Liu, A. Sudo, T. Endo, Synthesis and copolymerization of fully bio-based benzoxazines from guaiacol, furfurylamine and stearylamine, Green Chem. 14 (2012) 2799–2806.

[36] A. Van, K. Chiou, H. Ishida, Use of renewable resource vanillin for the preparation of benzoxazine resin and reactive monomeric surfactant containing oxazine ring, Polymer 55 (2014) 1443–1451.

[37] C.F. Wang, C.H. Zhao, J.Q. Sun, S.Q. Huang, X.D. Liu, T. Endo, Synthesis and thermal properties of a bio-based polybenzoxazine with curing promoter, J. Polym. Sci., Part A: Polym. Chem. 51 (2013) 2016–2023.

[38] C.F. Wang, Y.C. Su, S.W. Kuo, C.F. Huang, Y.C. Sheen, F.C. Chang, Low-surface-free-energy materials based on polybenzoxazines, Angew. Chem. Int. Ed. 118 (2006) 2306–2309.

[39] C. Sawaryn, K. Landfester, A. Taden, Benzoxazine miniemulsions stabilized with polymerizable nonionic benzoxazine surfactants, Macromolecules 43 (2010) 8933–8941.

[40] A.A. Alhwaige, T. Agag, H. Ishida, S. Qutubuddin, Biobased chitosan/polybenzoxazine cross-linked films: preparation in aqueous media and synergistic improvements in thermal and mechanical properties, Biomacromolecules 14 (2013) 1806–1815.

[41] Y.H. Moon, S.H. Nam, J. Kang, Y.M. Kim, J.H. Lee, H.K. Kang, V. Breton, W.J. Jun, D. Ki- Park, A. Kimura, D. Kim, Enzymatic synthesis and characterization of arbutin

[42] glucosides using glucansucrase from Leuconostoc mesenteroides B-1299CB, Appl. Microbiol. Biotechnol. 77 (2007) 559–567.

[42] L. Orel, L. Kobrina, S. Sinelnikov, V. Boiko, V. Demchenko, S. Riabov, β-Cyclodextrin-containing pseudorotaxanes as building blocks for cross-linked polymers, J. Inclusion Phenom. Macrocycl. Chem. 92 (2018) 273–280.

[43] M. Okada, M. Kamachi, A. Harada, Preparation and characterization of inclusion complexes of poly(propylene glycol) with methylated cyclodextrins, J. Phys. Chem. B 103 (1999) 2607–2613.

[44] M. Okada, A. Harada, Preparation of â-cyclodextrin polyrotaxane: photodimerization of pseudo-polyrotaxane with 2-anthryl and triphenylmethyl groups at the ends of poly(propylene glycol), Org. Lett. 6 (2004) 361–364.

[45] S.C. Chan, S.W. Kuo, F.C. Chang, Synthesis of the organic/inorganic hybrid star polymers and their inclusion complexes with cyclodextrins, Macromolecules 38 (2005) 3099–3107.

[46] S.C. Chan, S.W. Kuo, H.S. She, H.M. Lin, H.F. Lee, F.C. Chang, Supramolecular aggregations through the inclusion complexation of cyclodextrins and polymers with bulky end groups, J. Polym. Sci., Part A: Polym. Chem. 45 (2007) 125–135.

[47] C.W. Tu, S.W. Kuo, F.C. Chang, Supramolecular self-assembly through inclusion complex formation between poly (ethylene oxide-b-N-isopropylacrylamide) block copolymer and α-cyclodextrin, Polymer 50 (2009) 2958–2966.

[48] Y. Xie, X. Wang, X. Han, X. Xue, W. Ji, Z. Qi, J. Liu, B. Zhao, Y. Ozaki, Sensing of polycyclic aromatic hydrocarbons with cyclodextrin inclusion complexes on silver nanoparticles by surface-enhanced Raman scattering, Analyst 135 (2010) 1389–1394.

[49] M. Okada, Y. Kawaguchi, H. Okumura, M. Kamachi, A. Harada, Complex formation of cyclodextrins with poly(propylene glycol) derivatives, J. Polym. Sci., Part A: Polym. Chem. 38 (2000) 4839–4849.

[50] M. Giulbudagian, S. Hönzke, J. Bergueiro, D. Işık, F. Schumacher, S. Saeidpour, S. B. Lohan, M.C. Meinke, C. Teutloff, M. Schäfer-Korting, G. Yealland, B. Kleuser, S. Hedtrich, M. Calderón, Enhanced topical delivery of dexamethasone by β-cyclodextrin decorated thermoresponsive nanogels, Nanoscale 10 (2018) 469–479.

[51] A. Harada, Preparation and structures of supramolecules between cyclodextrins and polymers, Coord. Chem. Rev. 148 (1996) 115–133.

[52] Y.C. Lin, P.I. Wang, S.W. Kuo, Water-soluble, stable helical polypeptide-grafted cyclodextrin bioconjugates: synthesis, secondary and self-assembly structures, and inclusion complex with guest compounds, Soft Matter 8 (2012) 9676–9684.

[53] Y.C. Wu, S.W. Kuo, Synthesis and characterization of polyhedral oligomeric silsesquioxane (POSS) with multifunctional benzoxazine groups through click chemistry, Polymer 51 (2010) 3948–3955.

[54] T. Takeichi, T. Kawauchi, T. Agag, High performance polybenzoxazines as a novel type of phenolic resin, Polym. J. 40 (2008) 1121–1131.

[55] T. Agag, T. Takeichi, Synthesis and characterization of novel benzoxazine monomers containing allyl groups and their high-performance thermosets, Macromolecules 36 (2003) 6010–6017.

[56] H. Ishida, T. Agag, in: Handbook of Polybenzoxazine Resins, Elsevier, Amsterdam, 2011.

[57] A. Harada, M. Okada, J. Li, M. Kamachi, Preparation and characterization of inclusion complexes of polypropylene glycol) with cyclodextrins, Macromolecules 28 (1995) 8406–8411.

[58] M. Ohmura, Y. Kawahara, K. Okude, Y. Hasegawa, M. Hayashida, R. Kurimoto, A. Kawaguchi, Electron microscopic observations of inclusion complexes of α-,β-, and γ-cyclodextrins, Polymer 45 (2004) 6967–6975.

[59] X.Q. Guo, L.X. Song, F.Y. Du, Z. Dang, M. Wang, Important effects of lithium carbonate on stoichiometry and property of the inclusion complexes of polypropylene glycol and β-cyclodextrin, J. Phys. Chem. B 115 (2011) 1139–1144.

[60] L.X. Song, F.Y. Du, X.Q. Guo, S.Z. Pan, Formation, characterization, and thermal degradation behavior of a novel tricomponent aggregate of cyclodextrin, ferrocene, and polypropylene glycol, J. Phys. Chem. B 114 (2010) 1738–1744.